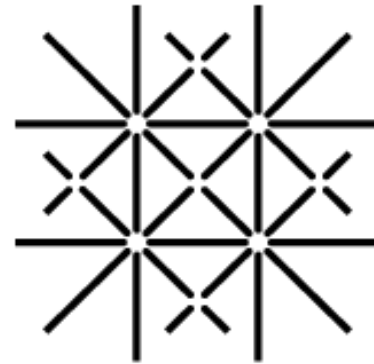


# SHUTTling IN SEMICONDUCTOR SYSTEM

---

Yang LIU  
11/04/2025



**University  
of Basel**

01

**Research Background**

02

Electron Spin Shuttling in Si/SiGe

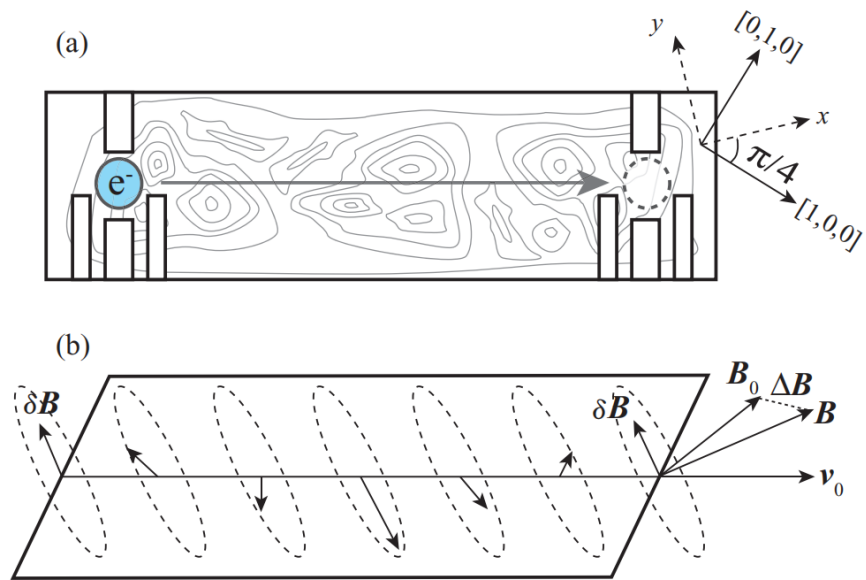
03

Hole Spin Shuttling in Ge/SiGe

04

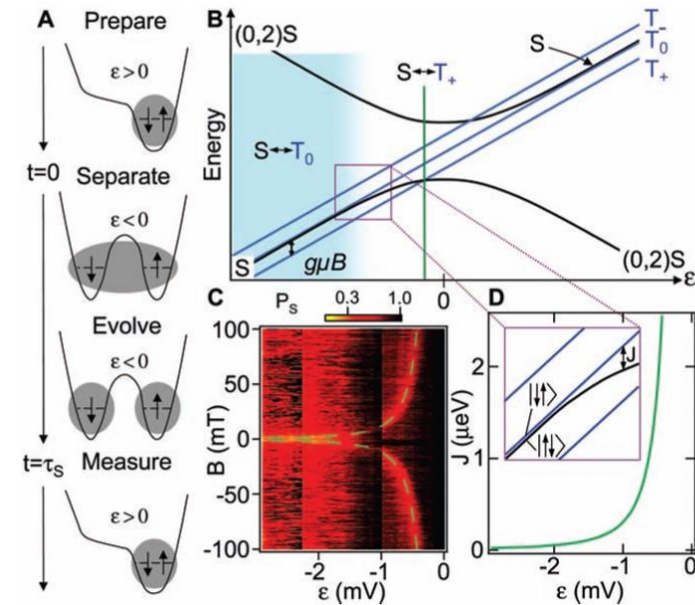
Conclusions and outlooks

# What is shuttling?



## How to couple the qubits?

- Short range (~10nm): SWAP gate
- Middle range (~10 $\mu$ m): surface acoustic wave, **shuttling**, resonant SWAP gate
- Long range (~100 $\mu$ m): resonator



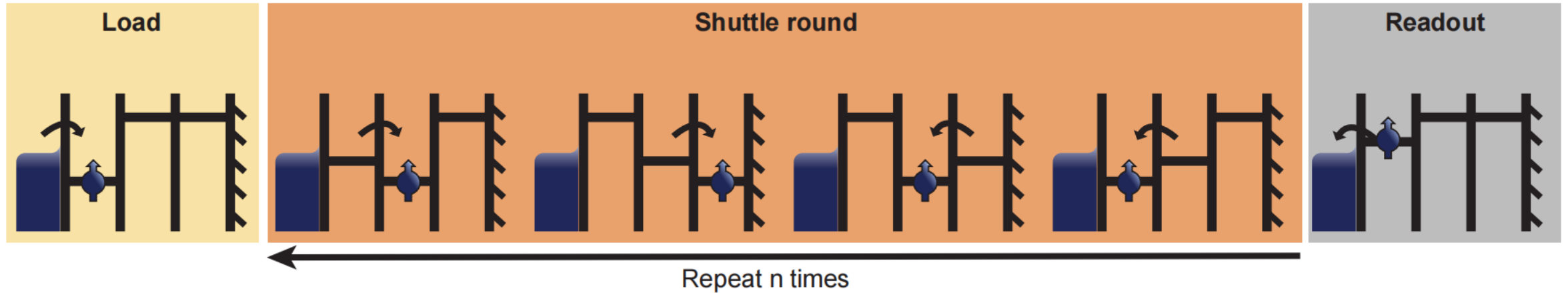
## Advantages of shuttling?

- No need for extra structure in device
- Increase the scalability
- Can be used to tune J between qubits

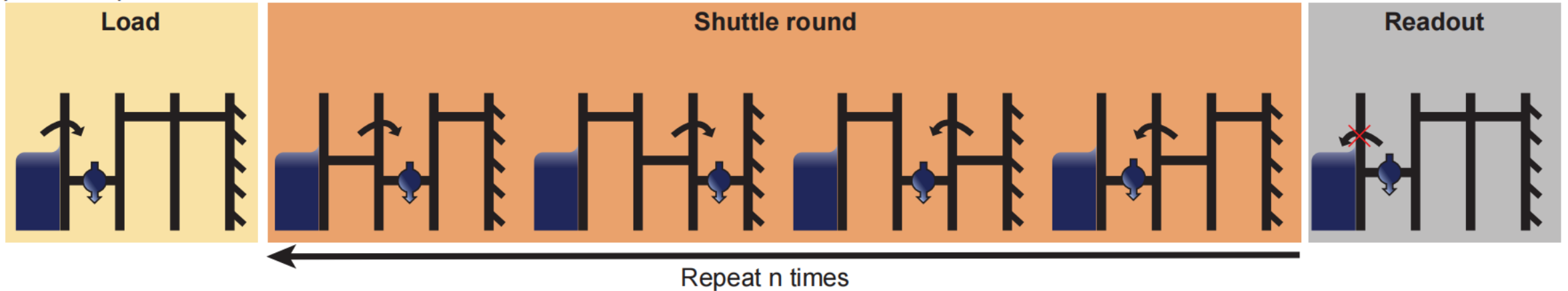
Year	Group	Charge / Spin	Material	QD	Reference
2017	T. Meunier (Grenoble)	Electron spin	AlGaAs-GaAs	Triangle 3 dots	Flentje et al., Nat. Commun 8, 501 (2017)
2019	Petta (Princeton)	Electron charge	<sup>28</sup> Si/SiGe	3*1	Mills et al., Nat. Commun 10, 1063 (2019)
2021	Dzurak (UNSW)	Electron spin	SiMOS	2*1	Yoneda et al., Nat. Commun 12, 4114 (2021)
2022	Tarucha (Riken)	Electron spin	<sup>28</sup> Si/SiGe	3*1	Noiri et al., Nat. Commun 13, 5740 (2022)
2023	Vandersypen (Delft)	Electron spin	<sup>28</sup> Si/SiGe	4*1	Zwerver et al., PRX Quantum 4, 030303 (2023)
2023	Schreiber (Aachen)	Electron spin	Natural Si/SiGe	8*1	Struck, et al., arXiv 2307.04897 (2023)
2024	Veldhorst (Delft)	Hole spin	Ge/SiGe	2*2	Floor van Riggelen-Doelman et al., Nat. Commun 15, 5716 (2024)
2024	Vandersypen (Delft)	Electron spin	<sup>28</sup> Si/SiGe	6*1	De Smet <sup>1</sup> , Y. Matsumot et al., arXiv:2406.07267 (2024)

# Two Types of Shuttling: Bucket-Brigade Mode

(e) Shuttle spin up

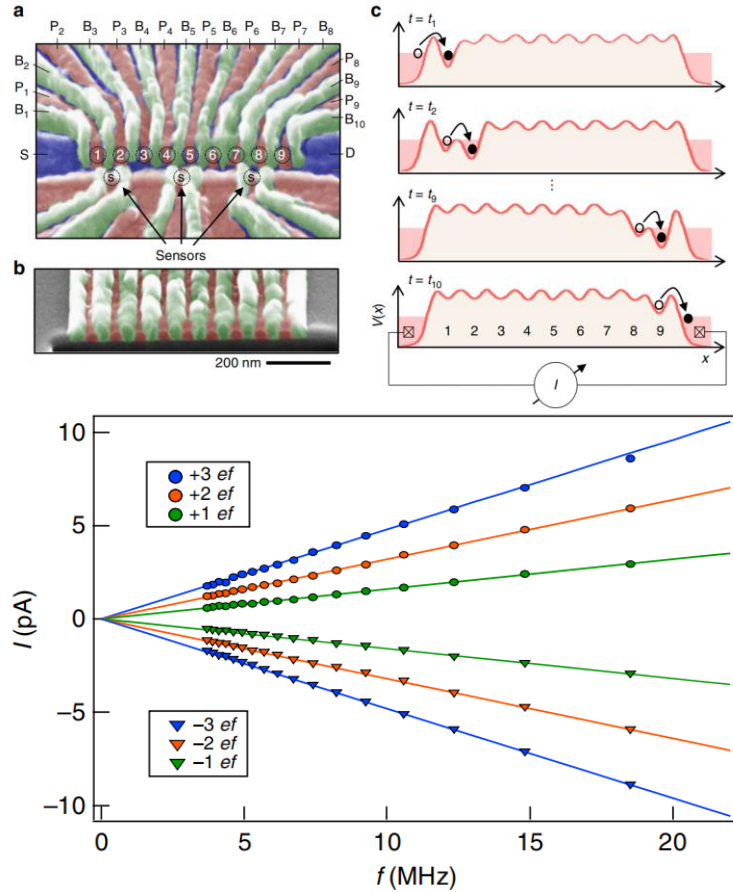


(f) Shuttle spin down

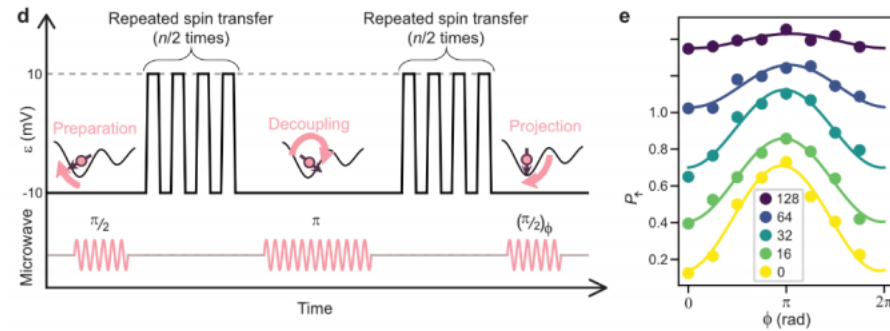
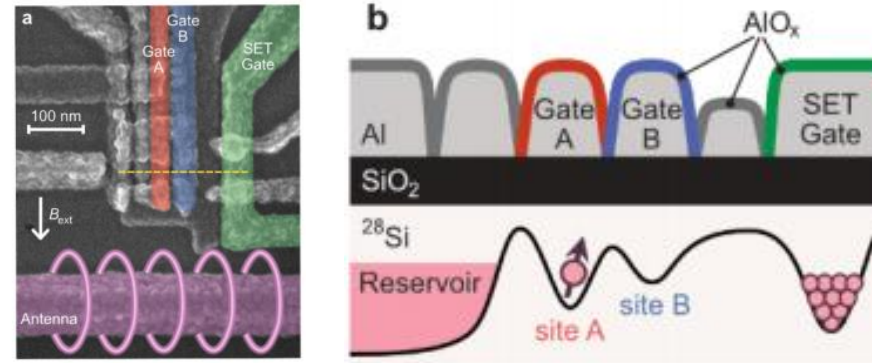


Bucket Brigade Mode: qubit shuttles across an array of tunnel-coupled static QDs

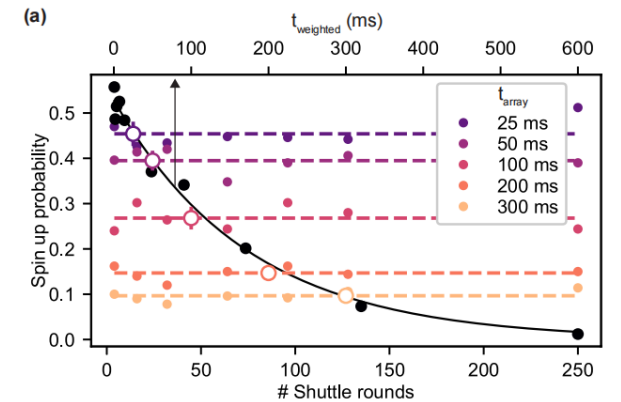
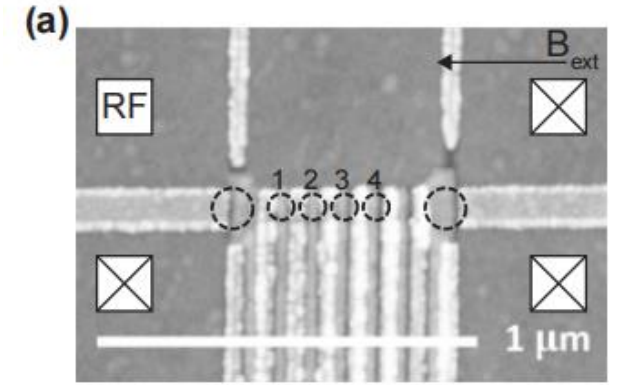
# Previous Work: Bucket-Brigade Mode



Current  $I$  measured as a function of frequency for electron charge shuttling  
 $I = nef, 3 \leq n \leq 3$   
 $V \approx 10 \text{ m/s}$

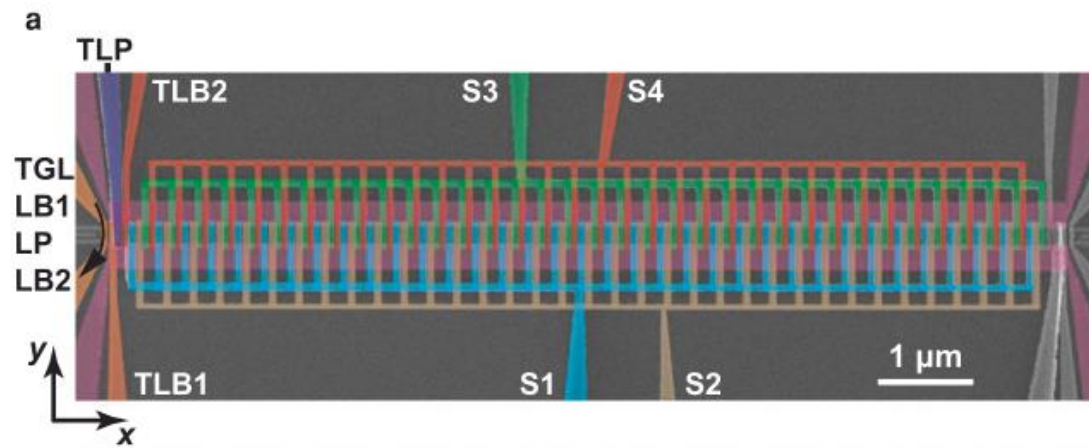
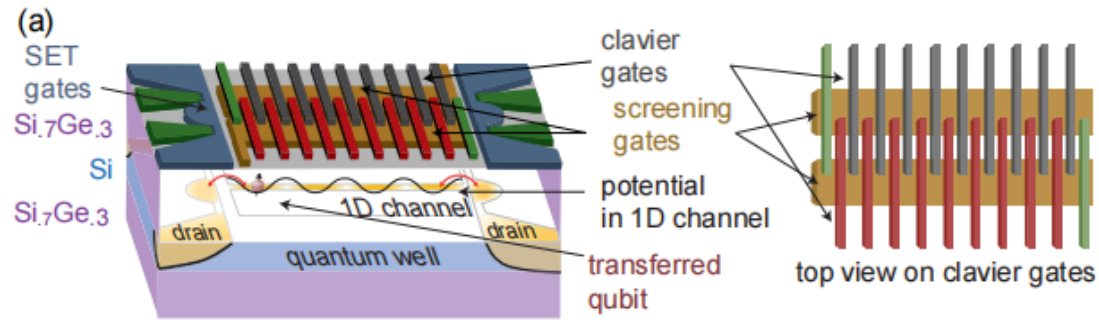


Shuttling through double quantum dots  
 Polarization transfer fidelity of 99.97%  
 Average coherent transfer fidelity of 99.4%  
 $V \approx 0.5 \text{ m/s}$



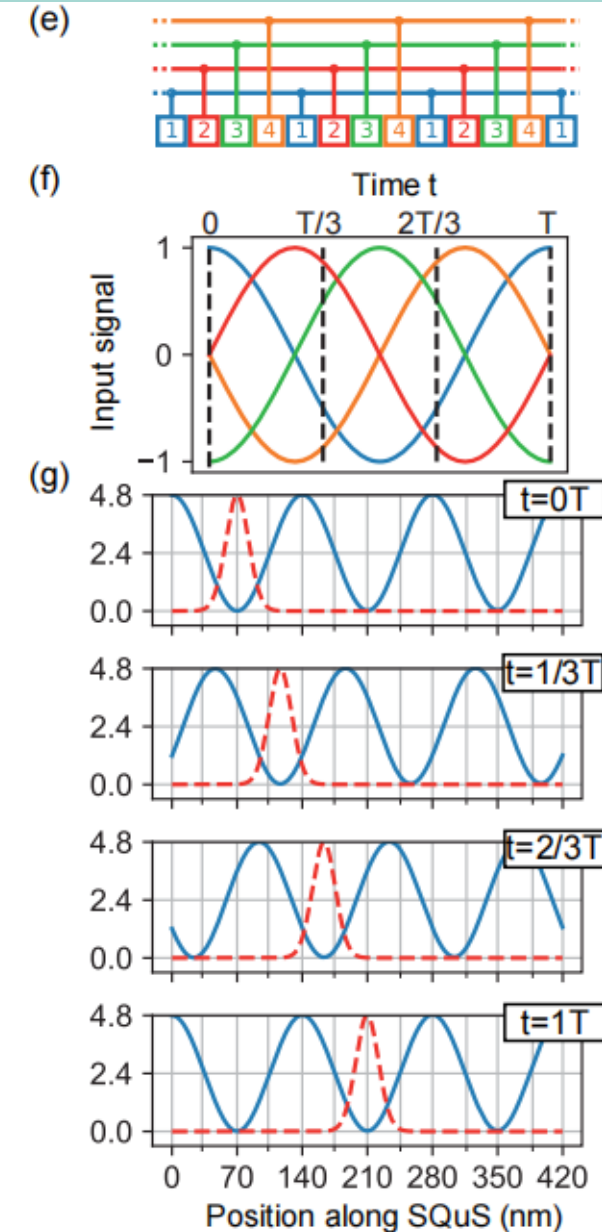
Shuttling through three quantum dots  
 Spin-flip probability per hop < 0.01%  
 $V \approx 0.004 \text{ m/s}$

# Two Types of Shuttling: Conveyor-Belt Mode



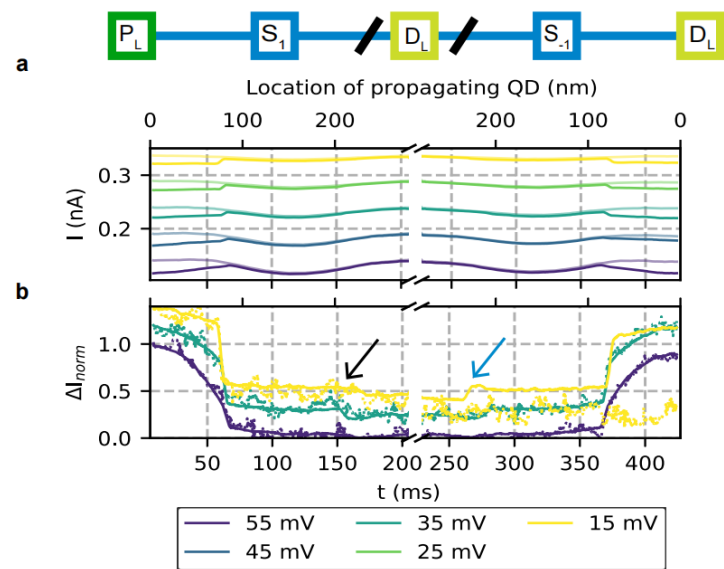
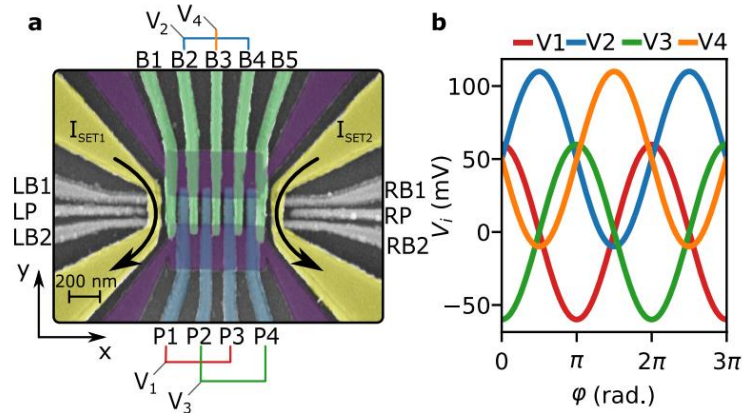
Spin shuttles using a moving potential wave:

- A series of electrostatic gates generate a traveling wave potential that traps and transports electrons sequentially.
- The wave moves at a controlled speed, ensuring electrons are shuttled without losing their quantum state

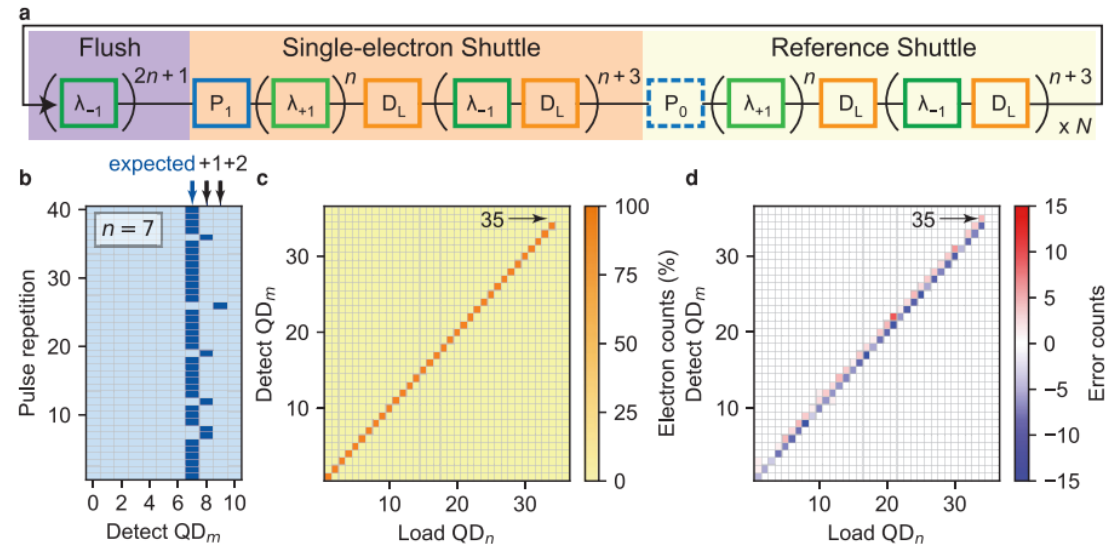
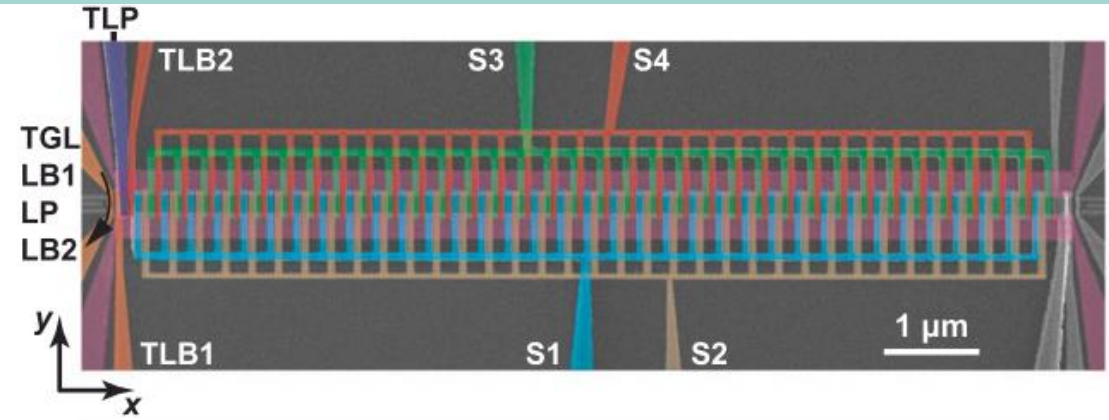


$$V_{si}(\tau_S) = U_i \cdot \sin(2\pi f \tau_S + \phi_i) + C_i$$

# Previous Work: Conveyor-Belt Mode



Single-electron shuttling fidelity is 99.42 %  
 $V \approx 1.4 \mu\text{m/s}$



The fidelity of the single-electron shuttle is  $(99.7 \pm 0.3)\%$   
 Total shuttling distance is  $19 \mu\text{m}$   
 $V \approx 10 \mu\text{m/s}$

	Bucket-Brigade Mode	Conveyor-Belt Mode
Advantage	<ol style="list-style-type: none"><li>1. Relatively easy to fabricate</li><li>2. Faster speed and higher fidelity compared to CB in short region</li></ol>	<ol style="list-style-type: none"><li>1. Relatively low requirement for adiabatic transfer</li><li>2. More smooth qubit transfer, higher fidelity in principle</li><li>3. No predefined quantum dots</li></ol>
Disadvantage	<p>Potential disorder and non-uniformity make it difficult to ensure tunnel coupling is large enough</p> <p><b>Easier for us to achieve BB mode in NW system</b></p>	<ol style="list-style-type: none"><li>1. Potential disorder and non-uniformity make it difficult to ensure that the potential wells at each location have similar shapes.</li><li>2. The process requires strictly on the shuttle path fabrication, such as no defects.</li></ol>

---

01

Research Background

02

**Electron Spin Shuttling in Si/SiGe**

03

Hole Spin Shuttling in Ge/SiGe

04

Conclusions and outlooks

# Electron Spin Shuttling in Si/SiGe

## High-fidelity single-spin shuttling in silicon

M. De Smet<sup>1†</sup>, Y. Matsumoto<sup>1†</sup>, A.M.J. Zwerver<sup>1</sup>, L. Tryputen<sup>2</sup>, S.L. de Snoo<sup>1</sup>, S.V. Amitonov<sup>2</sup>, A. Sammak<sup>2</sup>, N. Samkharadze<sup>2</sup>, Ö. Gül<sup>2</sup>, R. N. M. Wasserman<sup>2</sup>, M. Rimbach-Russ<sup>1</sup>, G. Scappucci<sup>1</sup>, and L.M.K. Vandersypen<sup>1\*</sup>

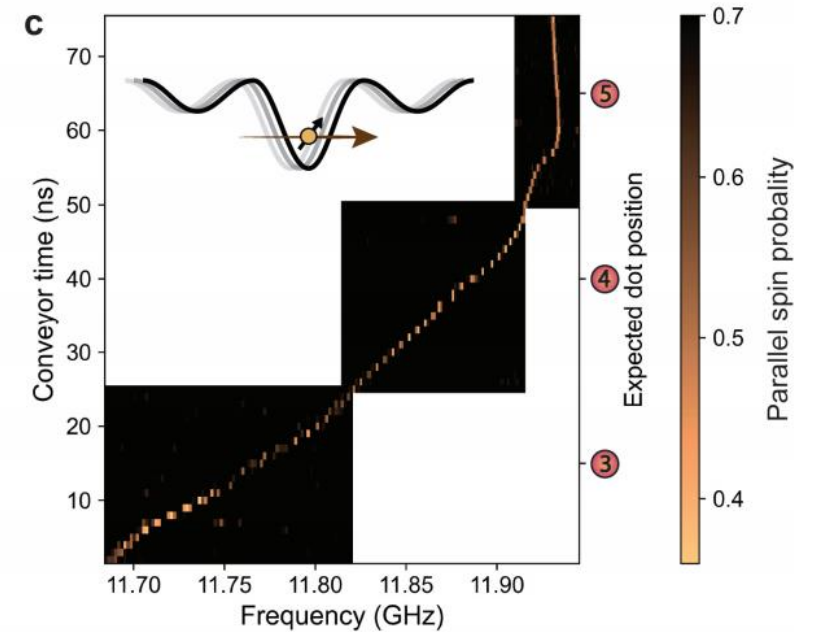
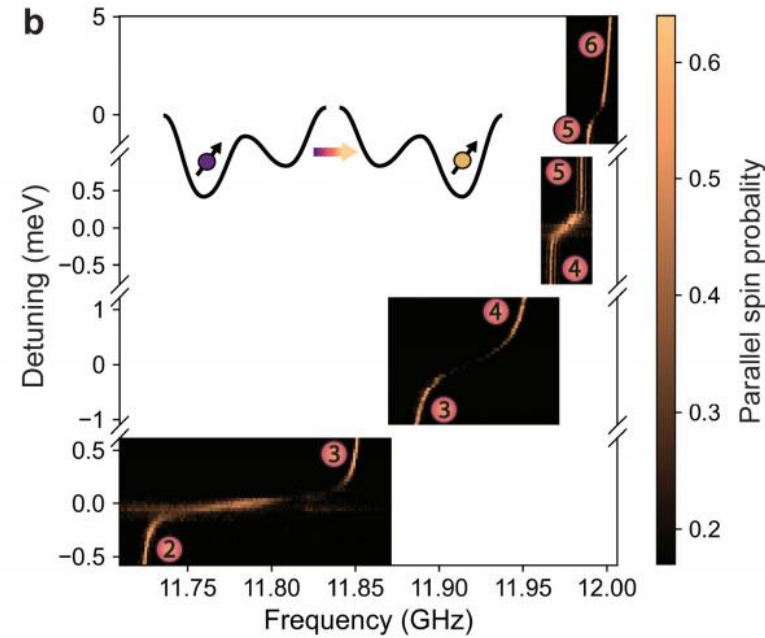
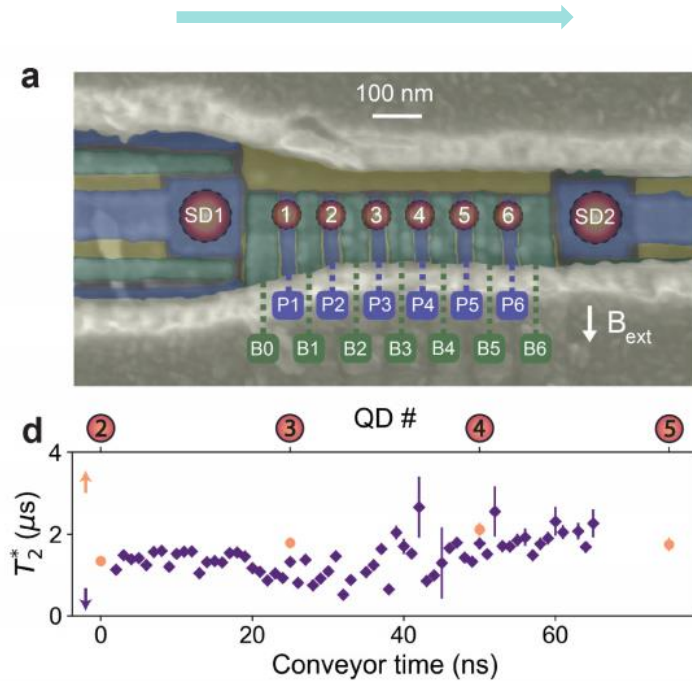
<sup>1</sup>QuTech and Kavli Institute of Nanoscience, Delft University of Technology, Lorentzweg 1, 2628 CJ Delft, The Netherlands

<sup>2</sup>QuTech and Netherlands Organization for Applied Scientific Research (TNO), Delft, The Netherlands and

<sup>†</sup> These authors contributed equally

(Dated: June 12, 2024)

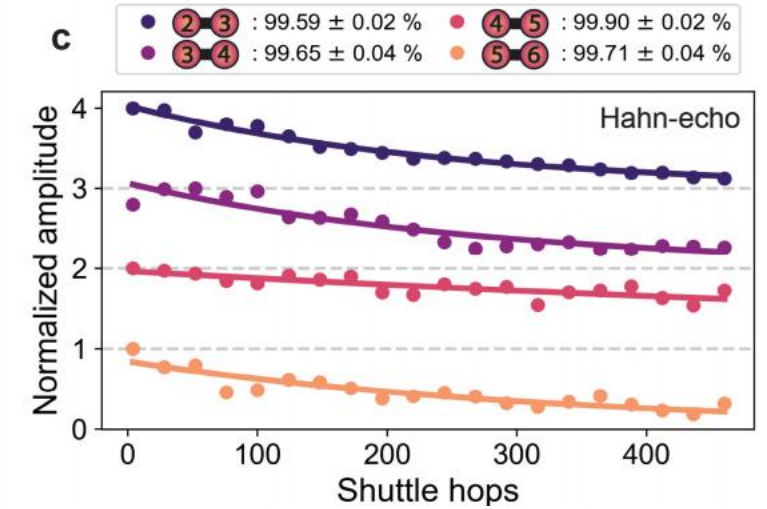
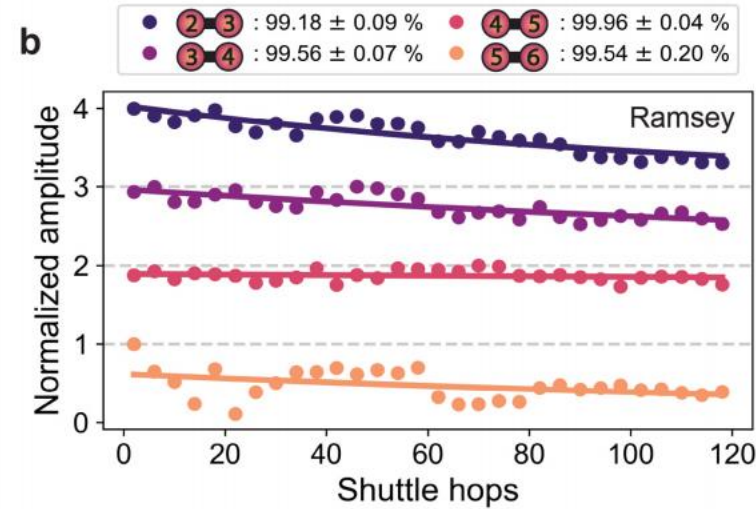
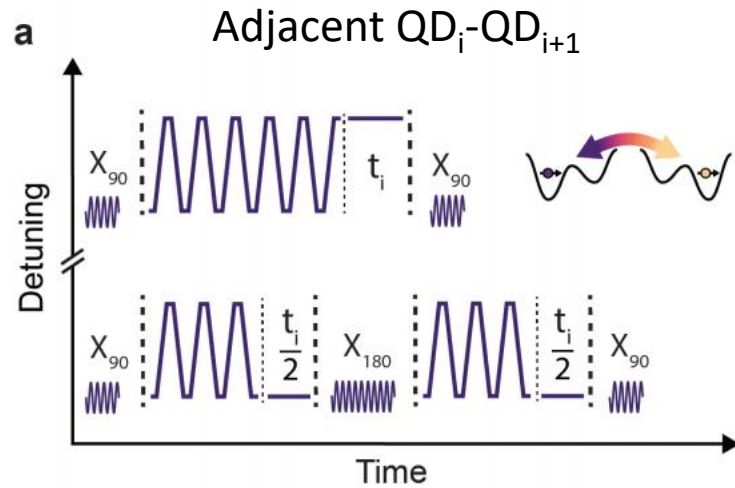
$T_2^*$  increases with decrease of  $B_{local}$



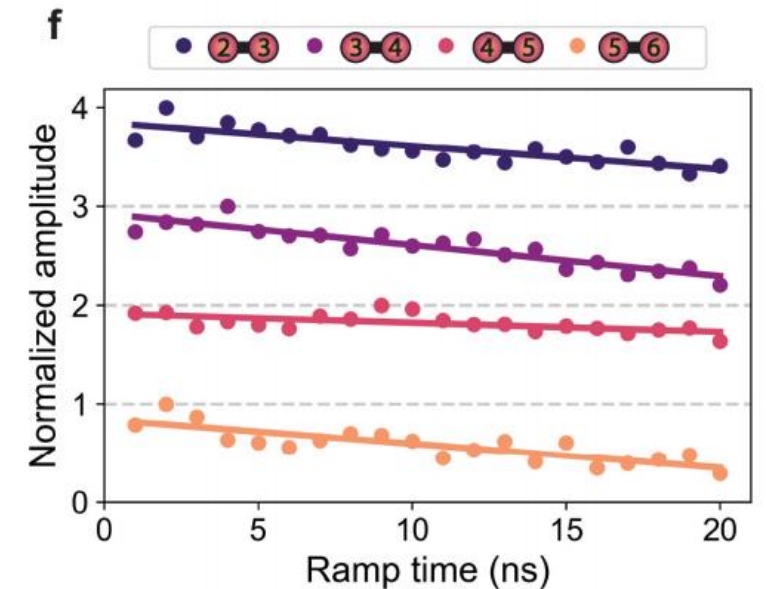
Spin dephasing time in the **gate-defined quantum dots** and in a **static two-tone conveyor**.

BB mode detuning dependence of spin resonance frequency

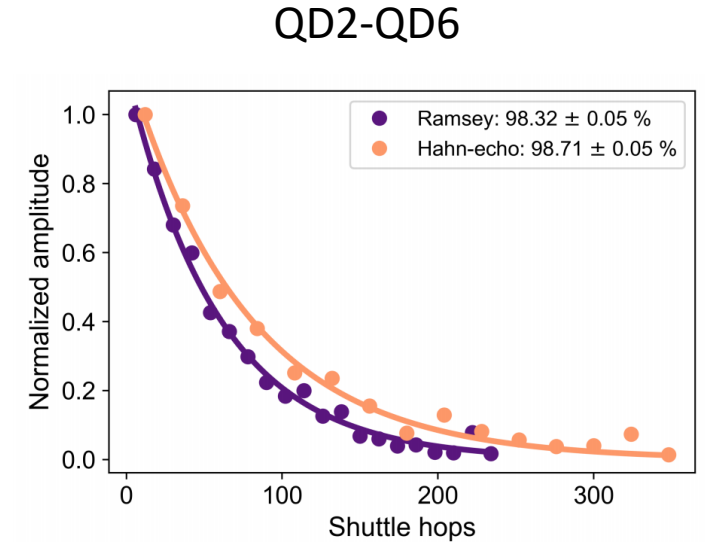
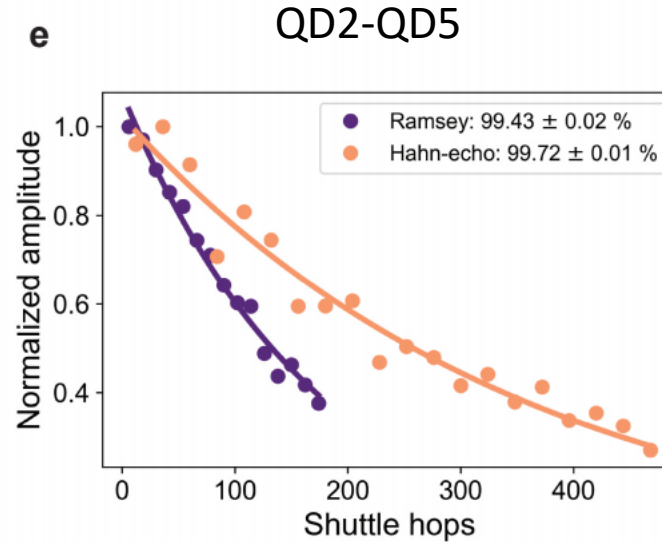
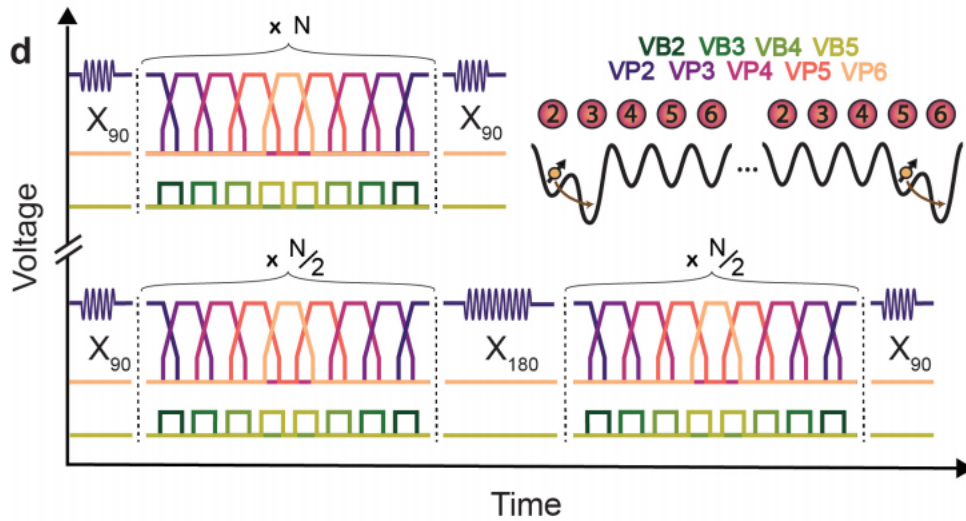
CV mode detuning dependence of spin resonance frequency



- Ramsey (top) and Hahn-echo (bottom) pulse sequences when shuttling repeatedly between sites of a DQD
- Ramsey and Hahn-echo fringe amplitude for each double dot with increasing number of shuttle hops
- Normalized Hahn-echo fringe amplitude after shuttling forth and back twice through a double dot as a function of the ramp time



# BB shuttling

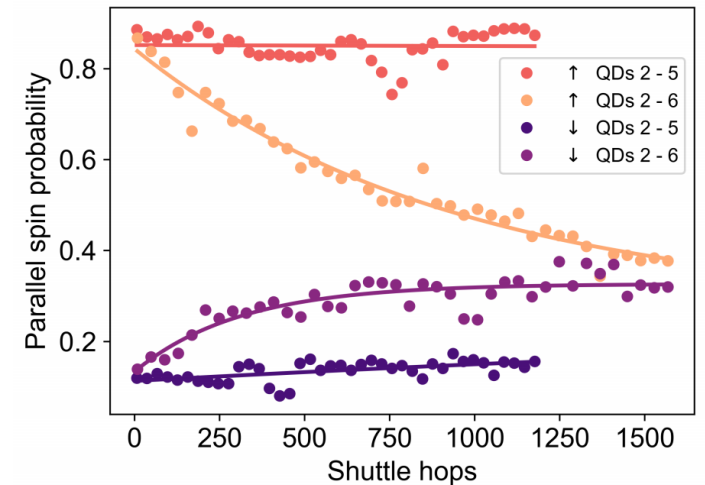


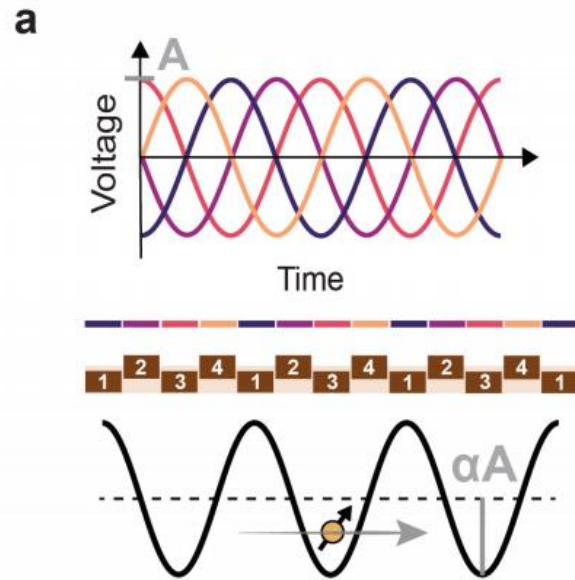
- B5 has a low lever arm of gate B5 and a small charging energy in QD5, needs more voltage to tune.
- Speculation: the small orbital energy could induce diabatic charge excitations. The artificial SOI from the micromagnet also affects the spin dephasing rate and spin relaxation rate during shuttling

$T_2^*$  of BB shuttling:  $1.04 \mu\text{s}$ , average  $T_2^* = 1.75 \mu\text{s}$  in the static dots.

## Several ways to increase the dephasing time:

- Shorter ramp time
- Higher detuning region, resonance frequency is highly sensitive to detuning fluctuations
- Lower the magnetic field, the loss of phase coherence increases with the Zeeman splitting difference.





Conventional conveyor approach:

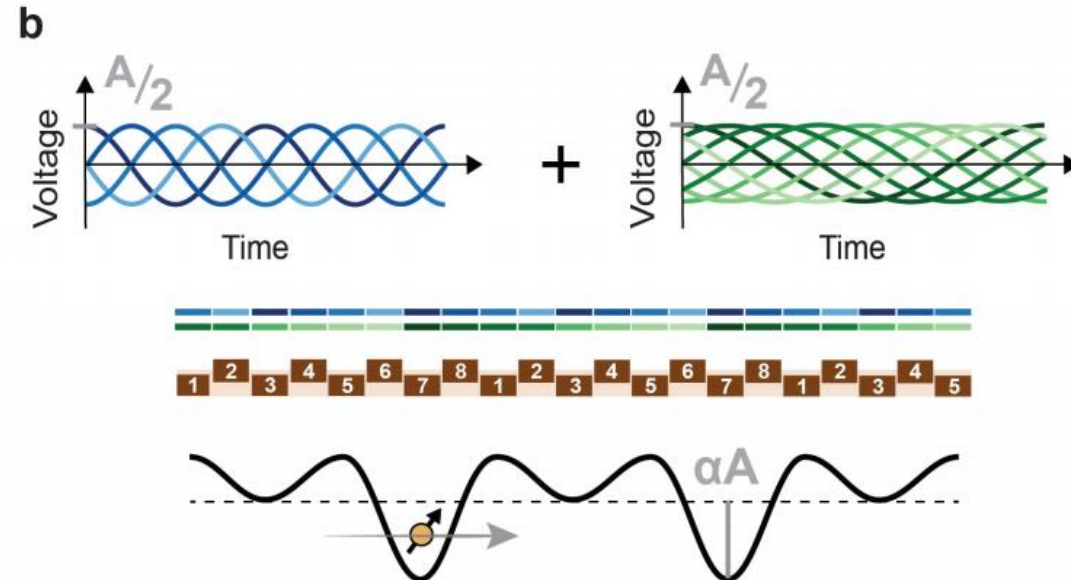
$$V_n(t) = V_n^{DC} - A \sin(2\pi ft - \phi_n)$$

$$\phi_n = \phi' + (n \bmod 4) \times \frac{\pi}{2}$$

$V_n^{DC}$ : DC voltage offset

$f$ : conveyor frequency

$\phi'$ : phase offset



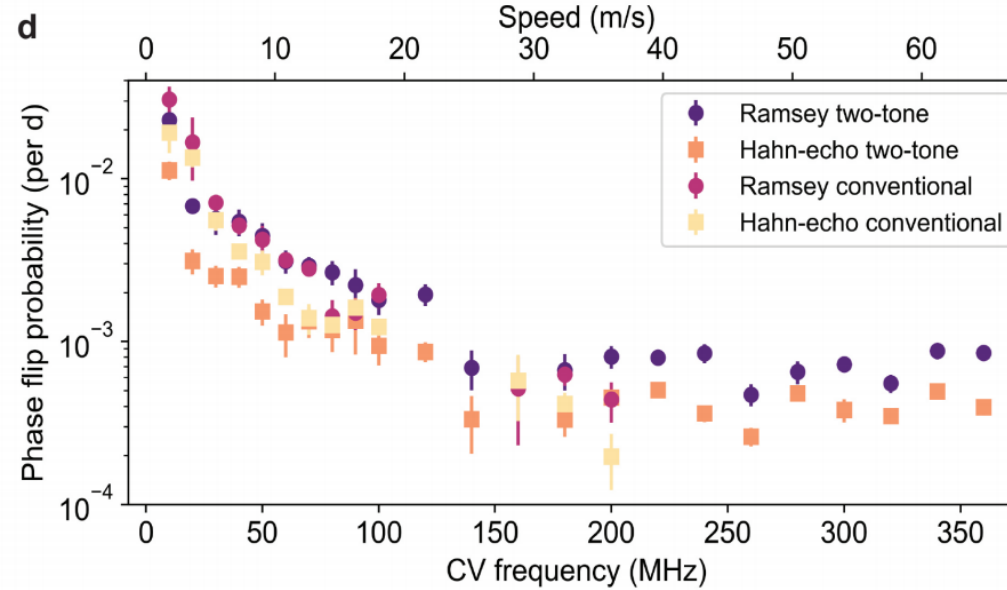
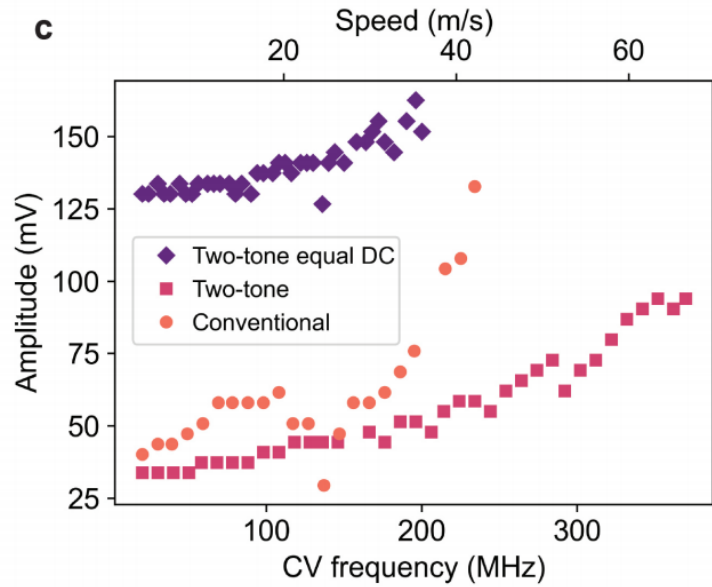
Two-tone conveyor approach:

$$V_n(t) = V_n^{DC} - \frac{A}{2} [\sin(2\pi ft - \phi_n) + \sin(\pi ft - \theta_n)]$$

$$\phi_n = \phi' + (n \bmod 4) \times \frac{\pi}{2}$$

$$\theta_n = \frac{\phi'}{2} + (n + 1 \bmod 8) \times \frac{\pi}{4}$$

- Destructive interference at every second potential minimum strongly suppresses charge leakage to neighbouring moving dots during shuttling
- Amplitude applies on barriers should be 1.4 times larger that of plungers

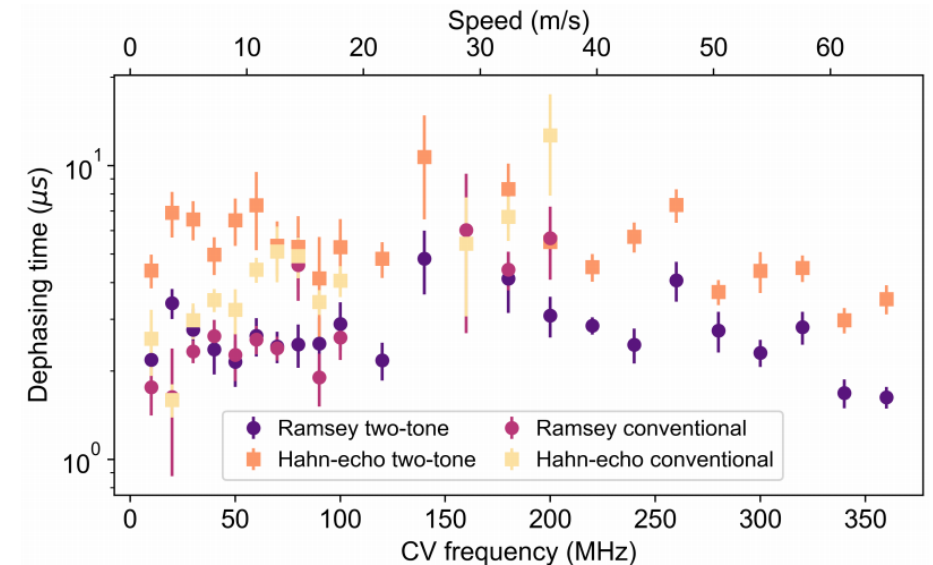


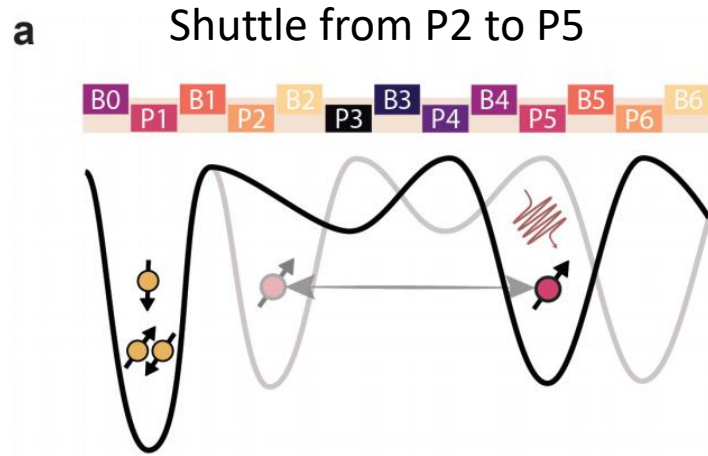
Conventional:  $V_n(t) = V_n^{DC} - A \sin(2\pi f t - \phi_n)$

Two-tone:  $V_n(t) = V_n^{DC} - \frac{A}{2} [\sin(2\pi f t - \phi_n) + \sin(\pi f t - \theta_n)]$

Two-tone equal DC:  $V_n(t) = V^{DC} - \frac{A}{2} [\sin(2\pi f t - \phi_n) + \sin(\pi f t - \theta_n)]$

Faster transfer means the spin has less time to dephase while transferring.  
The reason why P saturates after 150MHz is still unclear





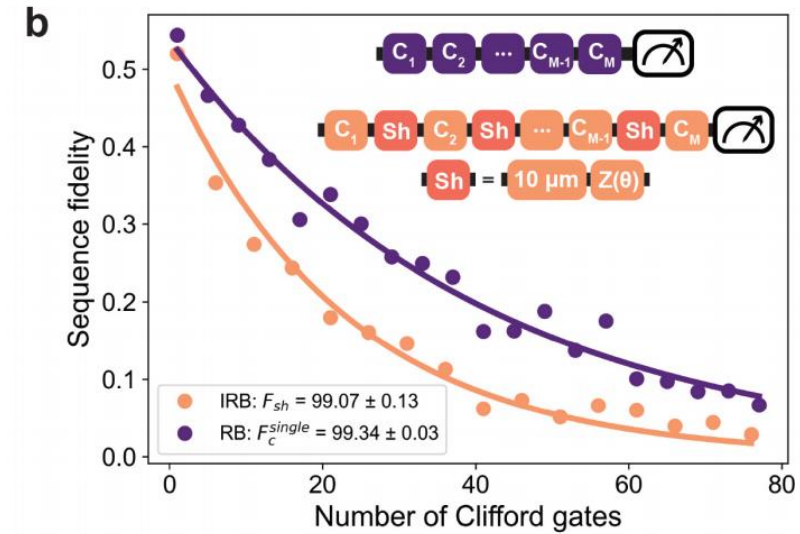
$$f_{CV} = 300 \text{ MHz}$$

$$t_{sh} = 4 \text{ ns}$$

$$N = 23$$

$$T_{total} = 184 \text{ ns}$$

$$D_{sh} = 2Nf_{CV}t_{sh}2d = 9.936 \mu\text{m}$$



Over a plunger-to-plunger distance:  $F = 99.99\%$

Calculation:

Single qubit gate fidelity:  $F = 99.34\%$

Shuttling fidelity over  $10\mu\text{m}$ :  $F = 99.07\%$

Shuttling fidelity:  $N = \frac{10\mu\text{m}}{90\text{nm}} \sim 100$ , every hop  $F > 99.99\%$

01

Research Background

02

Electron Spin Shuttling in Si/SiGe

03

Hole Spin Shuttling in Ge/SiGe

04

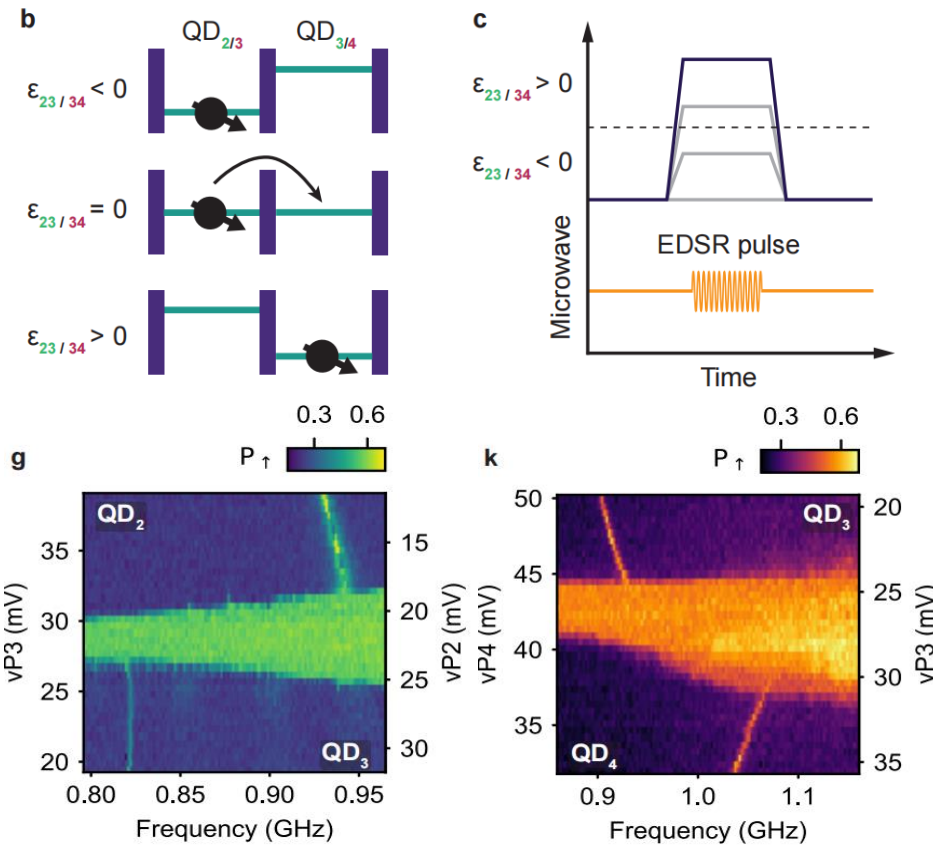
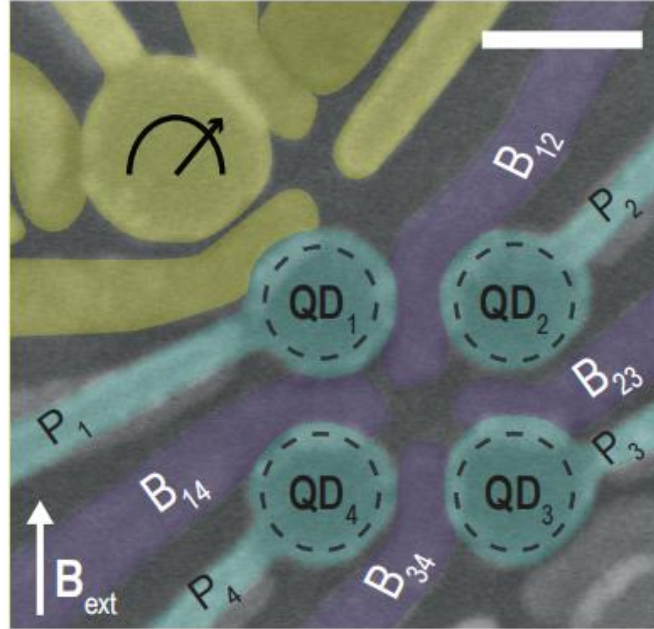
Conclusions and outlooks

## Hole Spin Shuttling in Ge/GeSi

Floor van Riggelen-Doelman,<sup>1</sup> Chien-An Wang,<sup>1</sup> Sander L. de Snoo,<sup>1</sup> William I. L. Lawrie,<sup>1</sup> Nico W. Hendrickx,<sup>1</sup> Maximilian Rimbach-Russ,<sup>1</sup> Amir Sammak,<sup>2</sup> Giordano Scappucci,<sup>1</sup> Corentin D eprez,<sup>1</sup> and Menno Veldhorst<sup>1</sup>

<sup>1</sup>QuTech and Kavli Institute of Nanoscience, Delft University of Technology, PO Box 5046, 2600 GA Delft, The Netherlands

<sup>2</sup>QuTech and Netherlands Organisation for Applied Scientific Research (TNO), Delft, The Netherlands (Dated: August 7, 2023)



	$T_1$ (ms)	$T_2^*$ (ns)	$T_2^{\text{Hahn}}$ ( $\mu\text{s}$ )
Qubit1	0.84	201	4.3
Qubit2	7.6	146	5.5
Qubit3	16.1	446	3.8
Qubit4	11.5	150	2.9

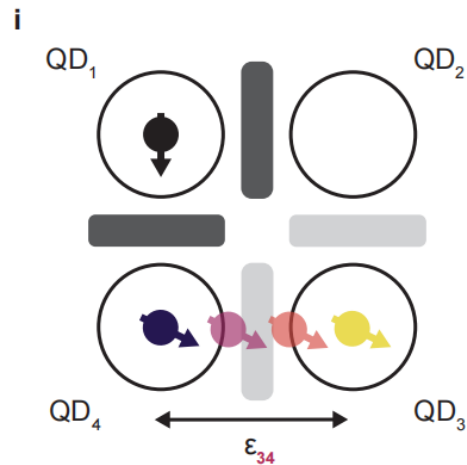
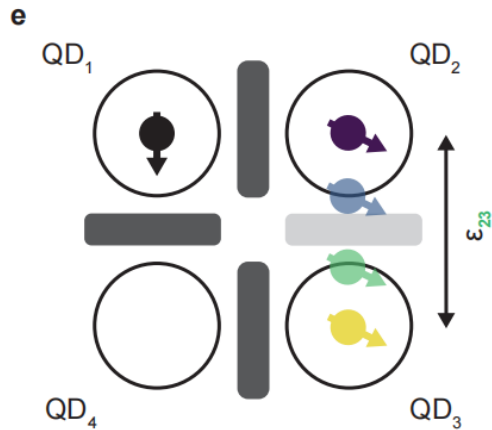
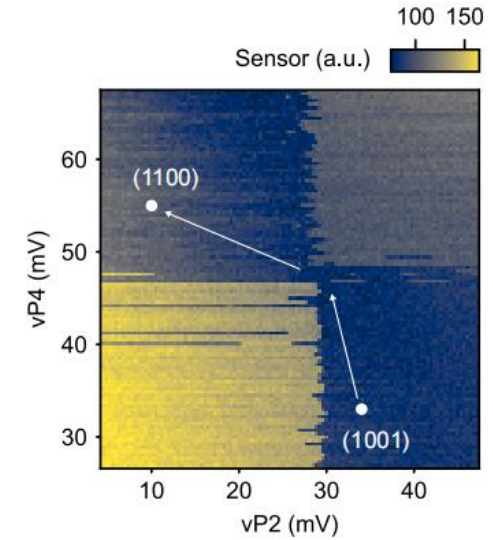
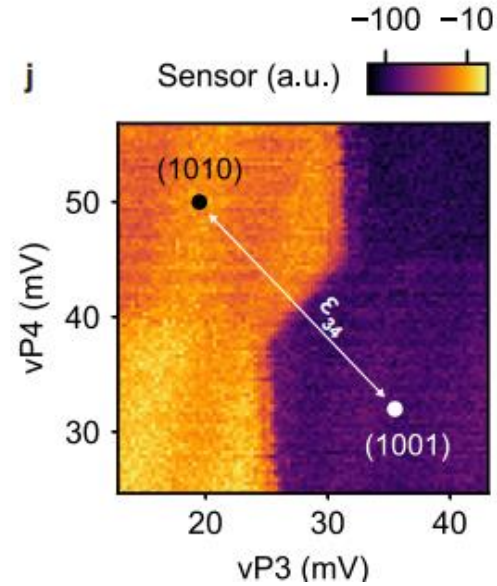
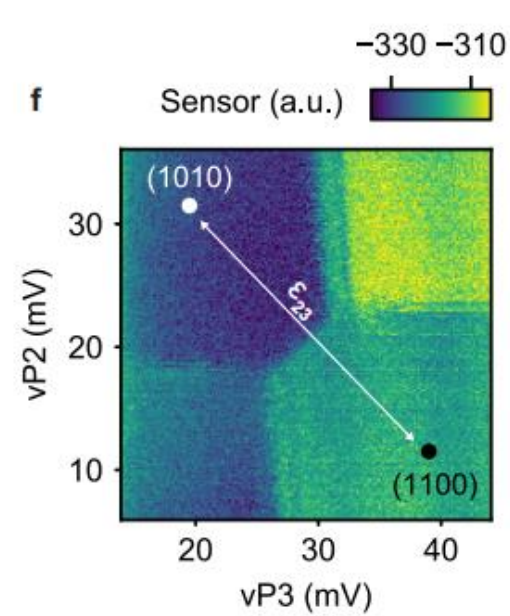
QD distance = 140 nm

Ge has small effective mass and high uniformity

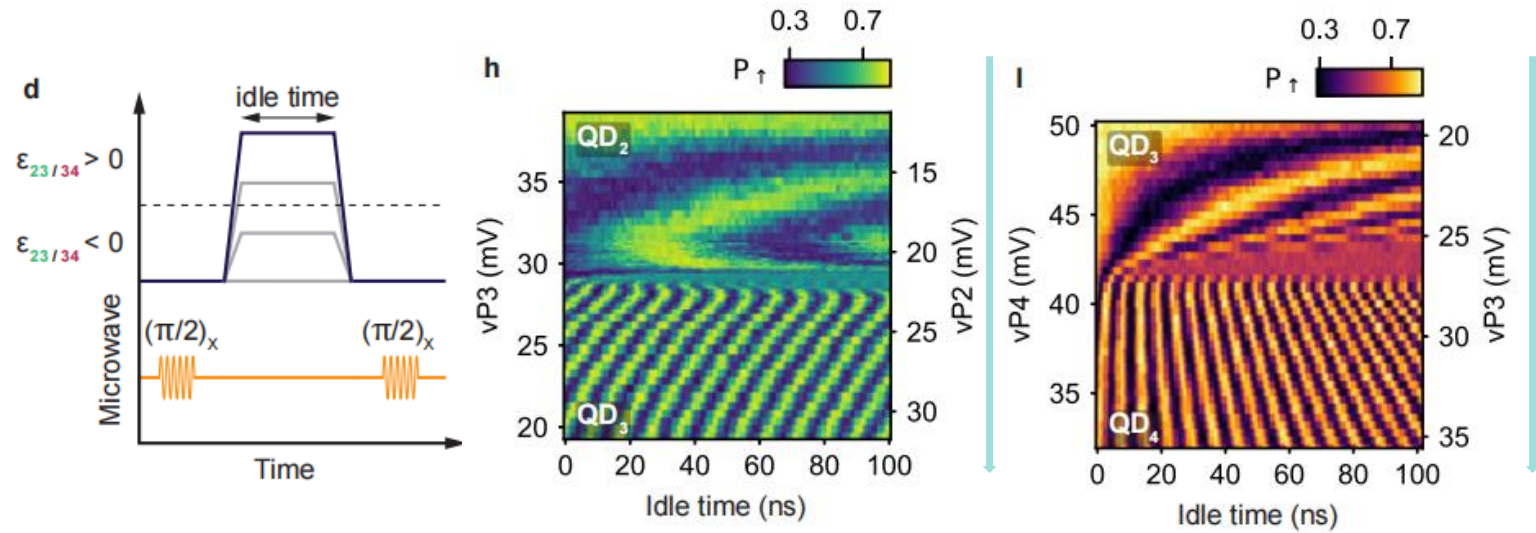
Hendrickx et al., Nature 591, 580–585 (2021)

- Change the detuning between two QDs to shuttle holes
- Pulses used for the shuttling, EDSR pulse lasts 4  $\mu\text{s}$
- We use the change of Larmor frequency to confirm the hole shuttles from one QD to another. The resonance frequency near the charge transition cannot be resolved due to a combination of effects

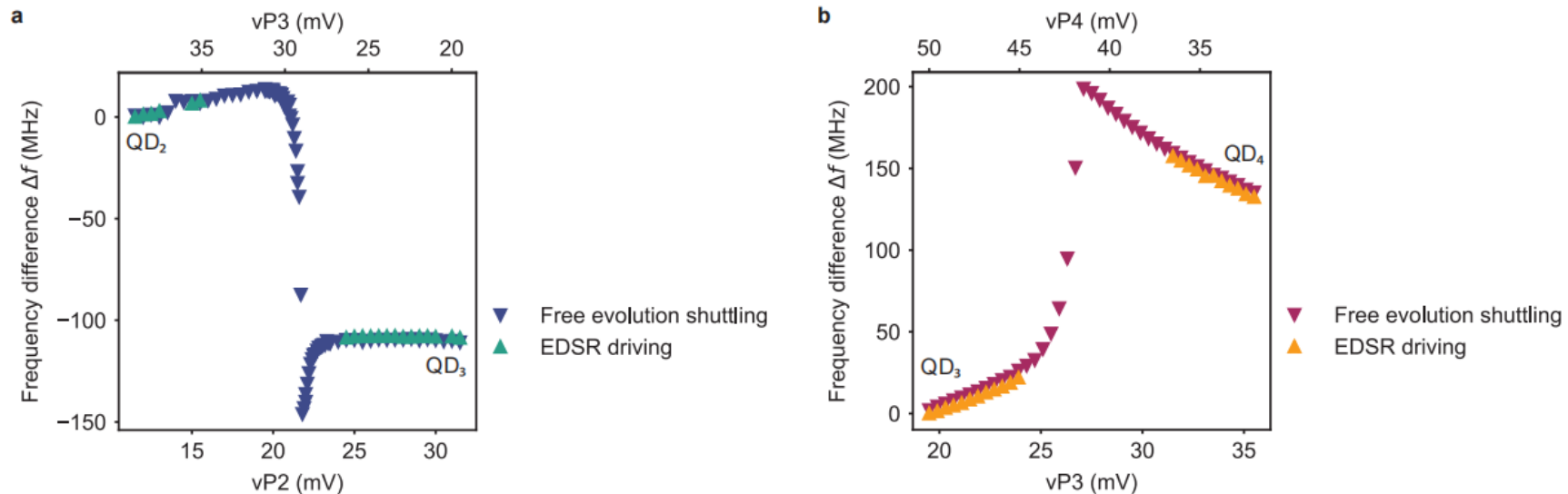
# Detuning Between QDs



- No clear interdot transition can be distinguished between QD2-QD4, the coupling between QD2 and QD4 is low
- We separately pulse to two parts to reduce the probability of exciting the (1,1,0,1) charge state during transition from (1,1,0,0) to (1,0,0,1)

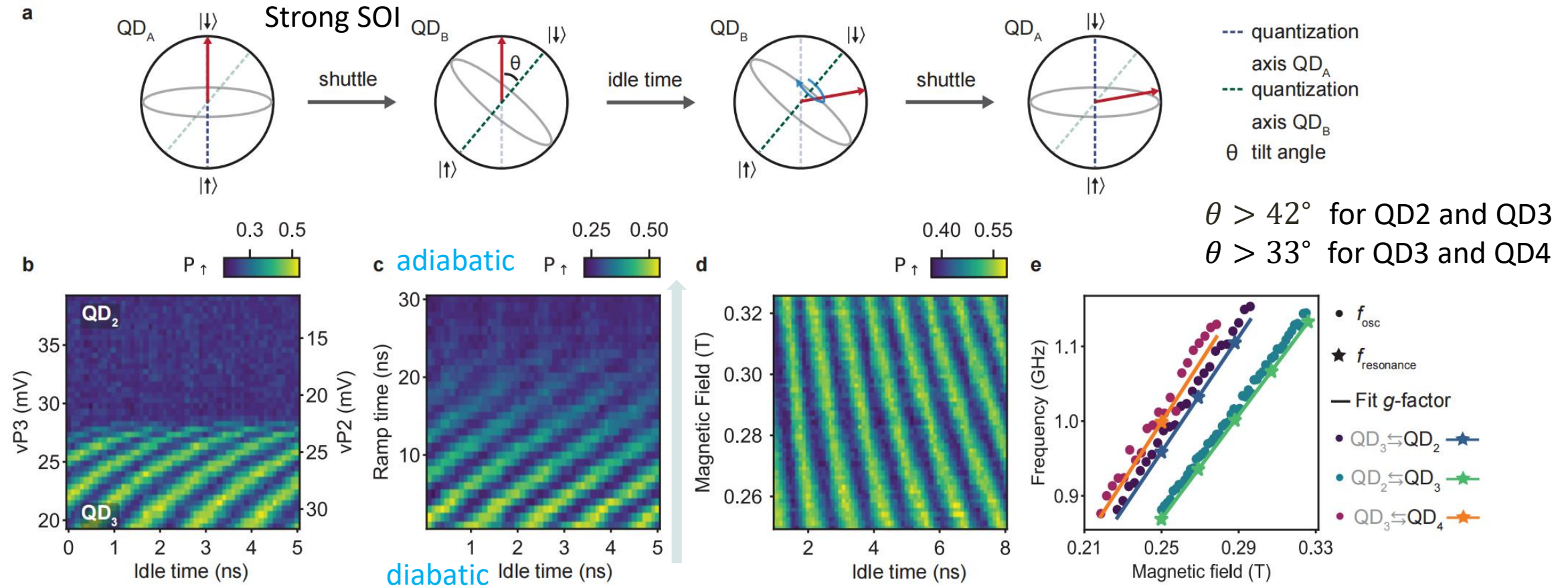


- Oscillation stripes: superposition state phase accumulation during idle time
- $f_{osc}$  changes with the difference in resonance frequency between the starting and end point in detuning



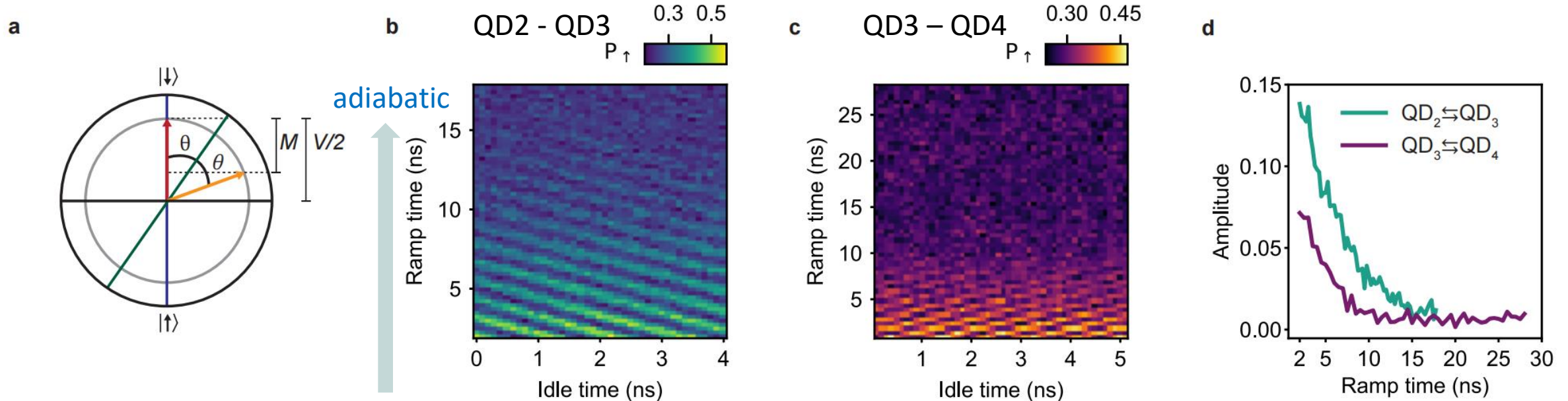
Evolution of the Larmor frequency for shuttling in DQD

# SOI Induced Quantization Axis Change



- Shuttle a spin down qubit between QD2 and QD3 diabatically ( $t_{ramp} = 4 \text{ ns}$ ), phase accumulates from the change of quantization axis
- Detuning is fixed, we increase the ramp time and the oscillation vanishes as increasing adiabatic.
- Magnetic-field dependence of the oscillations.  $f_{Larmor}$  increases linearly with magnetic field
- $f_{osc}$  increase linearly with magnetic field, matches Larmor frequency in QD

# Estimation of the Tilt Angle: Visibility



- Blue axis: quantization axis of QD1
- Green axis: quantization axis of QD2
- When spin down qubit shuttles to QD2, it will evolve freely around the green axis
- Orange arrow: after half a period, the state projection on the quantization axis of the QD1 differs maximally from that of the initial state
- $M$ : oscillation visibility
- $V$ : Rabi oscillation visibility

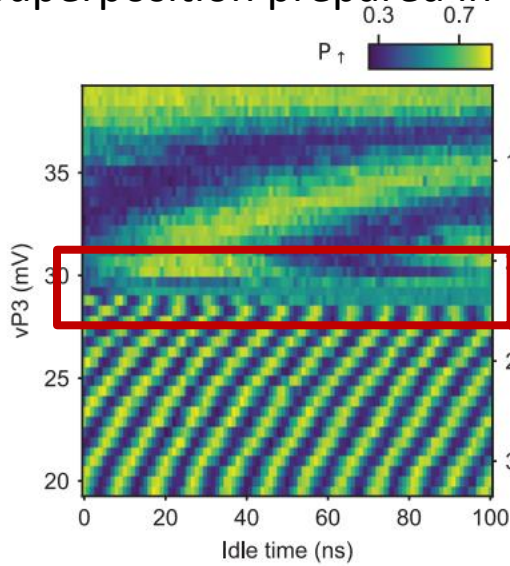
- Amplitudes  $\frac{M}{2}$  of the oscillations induced by the change in quantization axis as function of the pulse ramp time  $t_{ramp}$

$$\theta = \frac{1}{2} \arccos \left( 1 - 2 \frac{M}{V} \right), \quad 0 \leq \theta \leq \pi$$

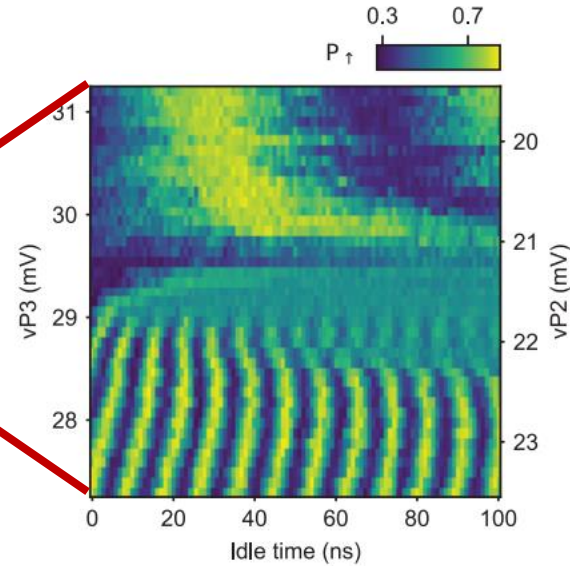
	QD2-QD3	QD3-QD4
$V$	0.61	0.48
$M$	0.28	0.14
$\theta$	$\geq 42^\circ$	$\geq 33^\circ$

# Estimation of the Tilt Angle: Four Level Model

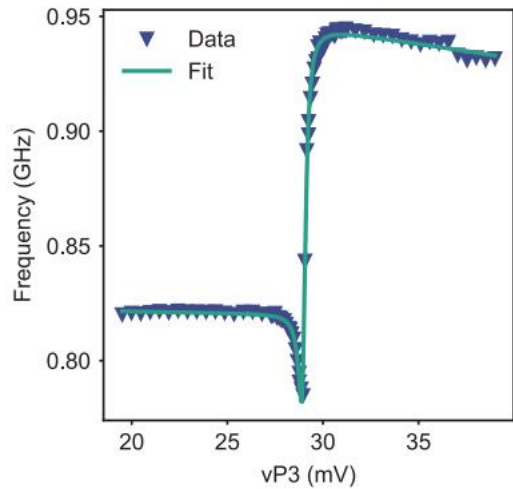
a Superposition prepared in QD2



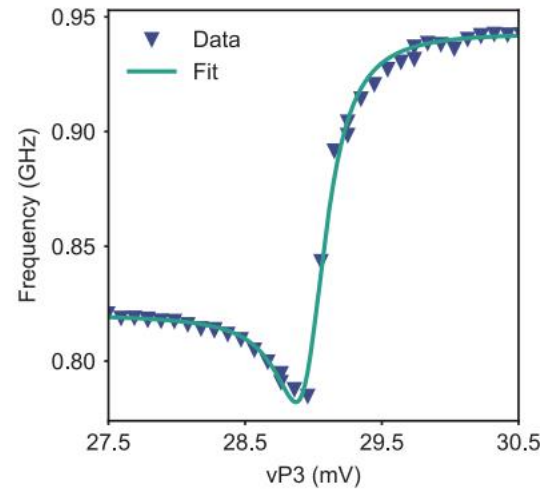
b



c



d



Four basis states  $\{|A, \uparrow_A\rangle, \{|A, \downarrow_A\rangle, \{|B, \uparrow_A\rangle, \{|B, \downarrow_A\rangle\}$   
 A, B: position of hole in QD<sub>A</sub> or QD<sub>B</sub>  
 $\uparrow_A$  and  $\downarrow_A$ : spin states in the frame of QD<sub>A</sub>  
 $\phi$  is tilt angle between 2 quantization axis

$$H_{\text{model}} = H_{\text{charge}} + H_{\text{Zeeman}} = \begin{pmatrix} \epsilon & 0 & t_c & 0 \\ 0 & \epsilon & 0 & t_c \\ t_c & 0 & -\epsilon & 0 \\ 0 & t_c & 0 & -\epsilon \end{pmatrix} + \frac{1}{2} B \mu_B \begin{pmatrix} g_A(\epsilon) & 0 & 0 & 0 \\ 0 & -g_A(\epsilon) & 0 & 0 \\ 0 & 0 & g_B(\epsilon) \cos(\theta) & g_B(\epsilon) \sin(\theta) e^{i\varphi} \\ 0 & 0 & g_B(\epsilon) \sin(\theta) e^{-i\varphi} & -g_B(\epsilon) \cos(\theta) \end{pmatrix}$$

$$f_L = \frac{\mu_B B}{h} \frac{\sqrt{(2\epsilon^2 + t_c^2)(g_A(\epsilon)^2 + g_B(\epsilon)^2) + 2\epsilon(g_B(\epsilon)^2 - g_A(\epsilon)^2)\sqrt{\epsilon^2 + t_c^2} + 2g_A(\epsilon)g_B(\epsilon)t_c^2 \cos(\theta)}}{2\sqrt{\epsilon^2 + t_c^2}},$$

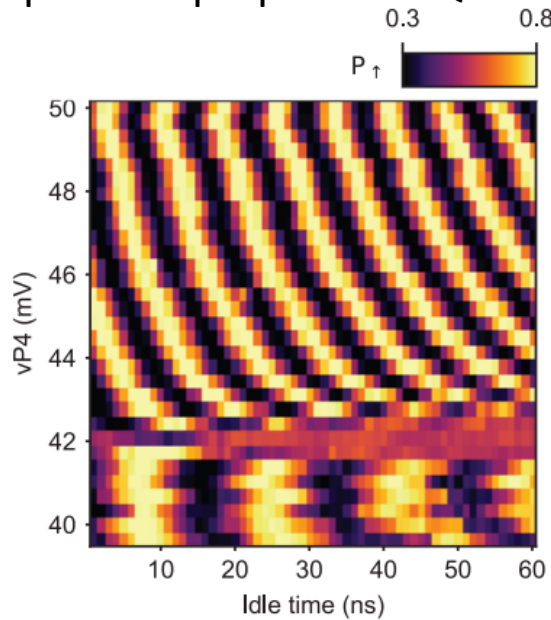
A **linear** dependence of g factor with vP3 in QD3

$$t_c = 8.7 \pm 0.3 \text{ GHz}$$

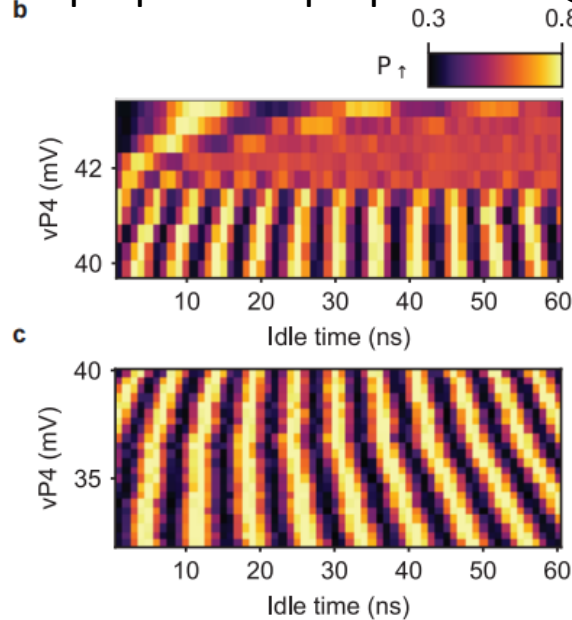
$$\theta_{23} = 51.8^\circ \pm 0.7^\circ$$

# Estimation of the Tilt Angle: Four Level Model

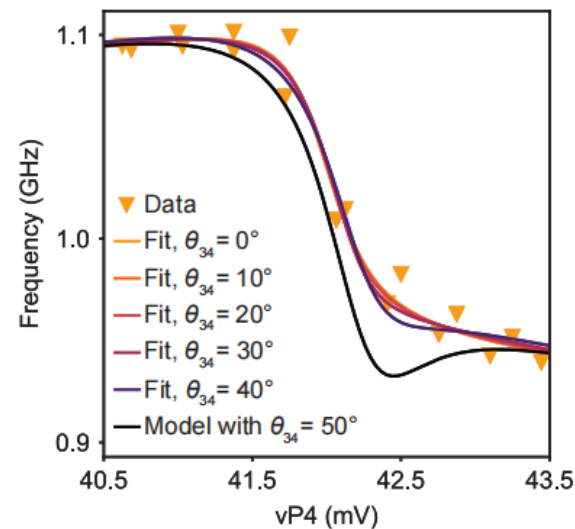
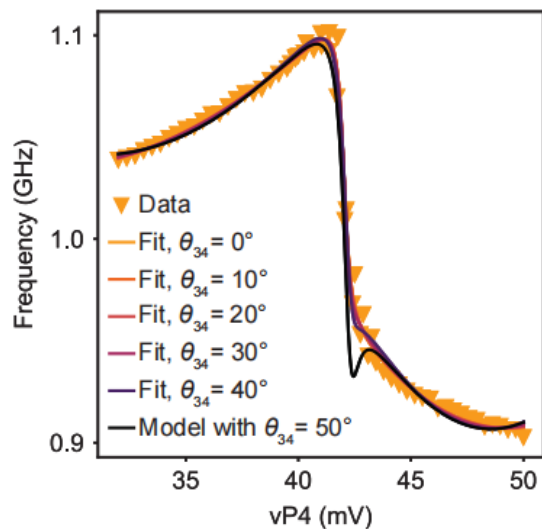
a Superposition prepared in QD4



b Superposition prepared in QD3



d



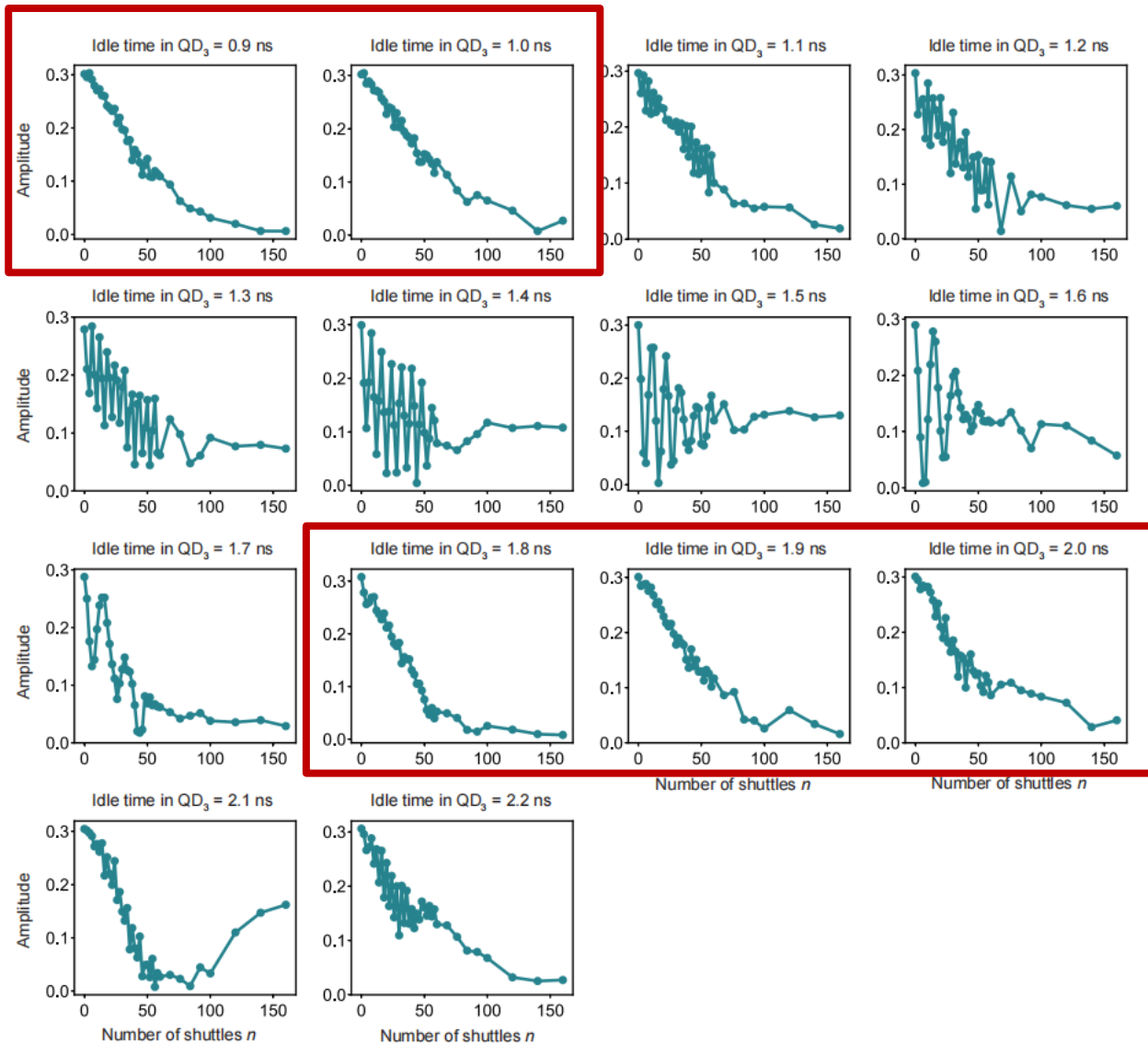
$$f_L = \frac{\mu_B B}{h} \frac{\sqrt{(2\epsilon^2 + t_c^2)(g_A(\epsilon)^2 + g_B(\epsilon)^2) + 2\epsilon(g_B(\epsilon)^2 - g_A(\epsilon)^2)\sqrt{\epsilon^2 + t_c^2} + 2g_A(\epsilon)g_B(\epsilon)t_c^2 \cos(\theta)}}{2\sqrt{\epsilon^2 + t_c^2}},$$

- Assume a **quadratic** dependence of the  $g$ -factor with the gate voltage
- $0^\circ \leq \theta \lesssim 40^\circ$ , the shape of  $f_L$  curve is nearly only determined by the tunnel coupling and the variation of the  $g$ -factor with  $vP4$ . This angles all fit well, cause large uncertainty.
- When  $\theta_{34} \geq 50^\circ$ , we see a minimum value in simulation but not in experiment

$$\theta = 40^\circ, t_c = 15 \pm 2 \text{ GHz}$$

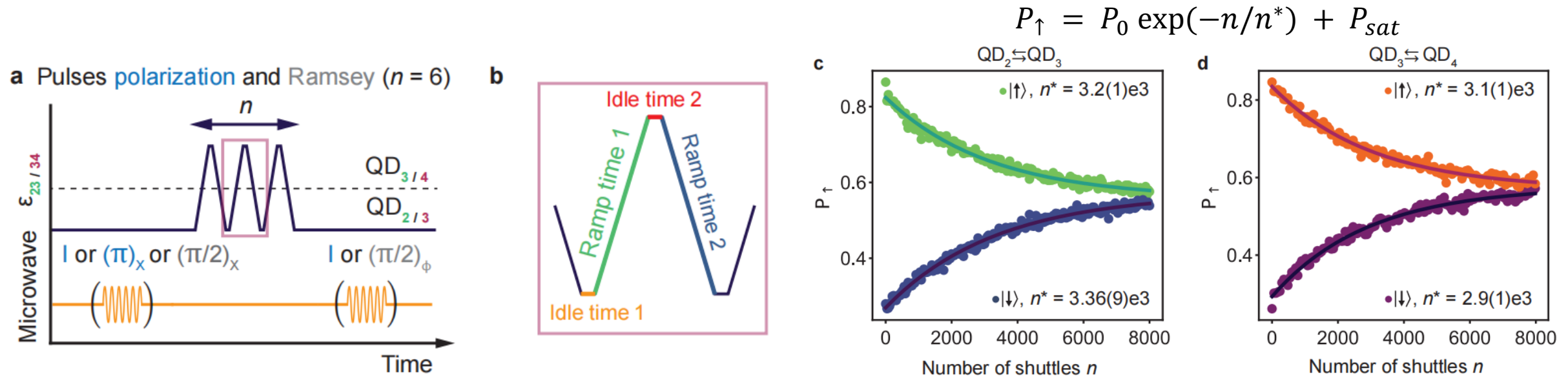
$$\theta = 30^\circ, t_c = 12 \pm 2 \text{ GHz}$$

# Optimization of the Shuttling Pulses



- Results of coherent shuttling experiments between QD2 and QD3 obtained using Ramsey sequences.
- For non-optimized idle times: oscillations of the amplitude and the amplitude can saturate to a non-zero value at large  $n$ .

$$t_{idle} = 0.95 \text{ ns}$$



## How to avoid unintended rotations:

- Transfer the qubit adiabatically. Ramp time can be up to tenths of ns, which are significant with respect to the decoherence time
- Qubit performs an integer number of  $2\pi$  rotations around the quantization axis of the respective quantum dot. This allows fast shuttling, ramp time 4ns and waiting time 1ns

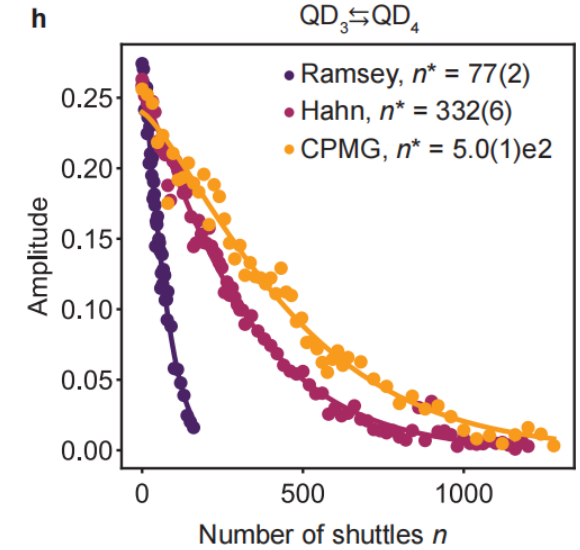
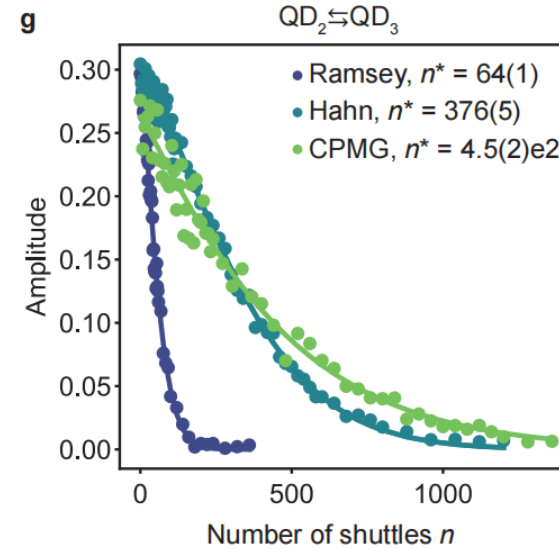
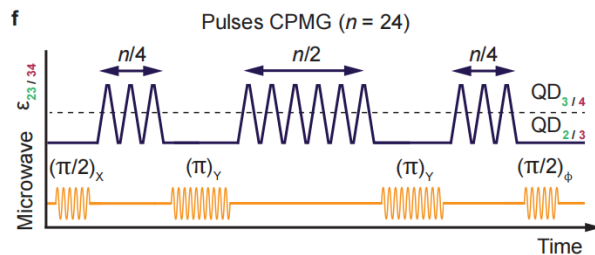
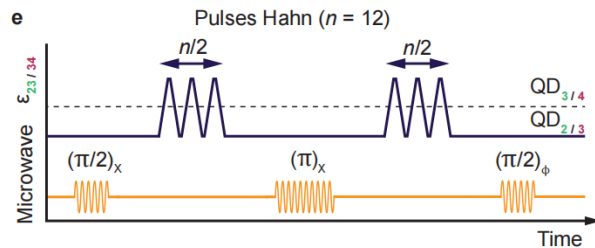
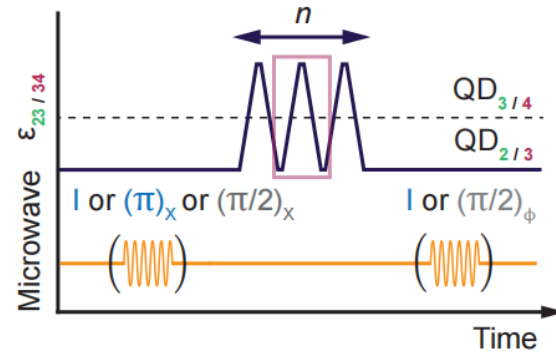
Fidelity for per hop:  $F = P_0 \exp\left(-\frac{1}{n^*}\right) \approx 99.97 \%$

This is similar to the fidelities reached in silicon devices <sup>[1,2]</sup>, despite anisotropic g-tensors induced by strong SOI in Ge

[1] Noiri et al., Nat. Commun 13, 5740 (2022)

[2] Yoneda et al., Nat. Commun 12, 4114 (2021)

a Pulses polarization and Ramsey ( $n = 6$ )



$$A(n) = A_0 \exp\left(-\left(\frac{n}{n^*}\right)^\alpha\right)$$

$$\alpha_{23} = 1.36 \pm 0.05, \alpha_{34} = 1.28 \pm 0.06$$

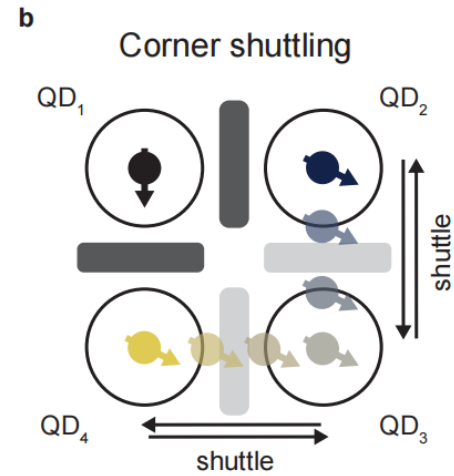
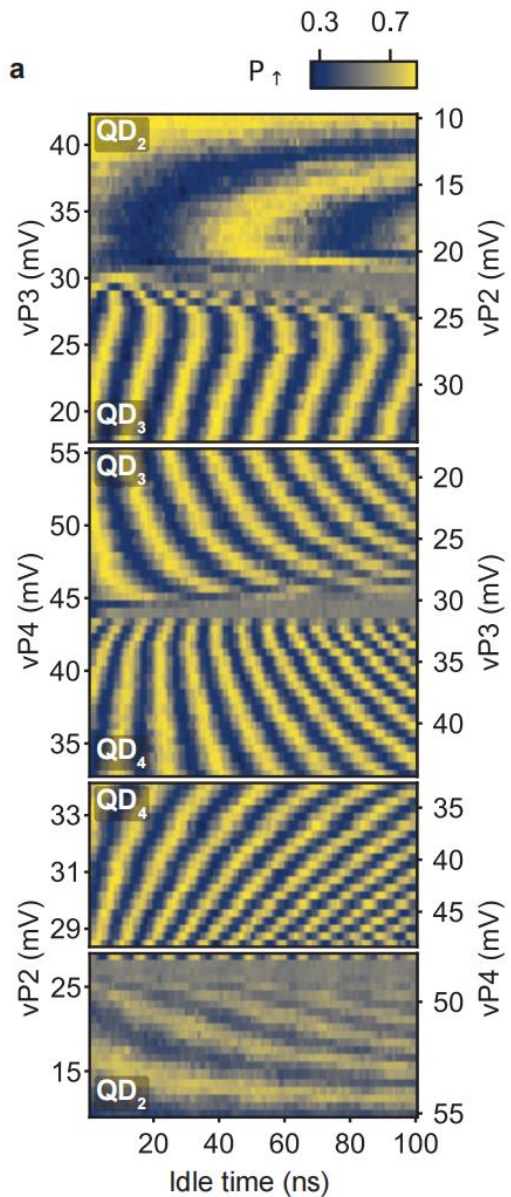
In SiMOS system<sup>[1]</sup> which has weaker SOI,  
 $n^* \approx 50$

	$n^*$	Effective length
Basis states	2230	312 $\mu m$
Coherent states	67	9 $\mu m$
Using echo pulse	350	49 $\mu m$

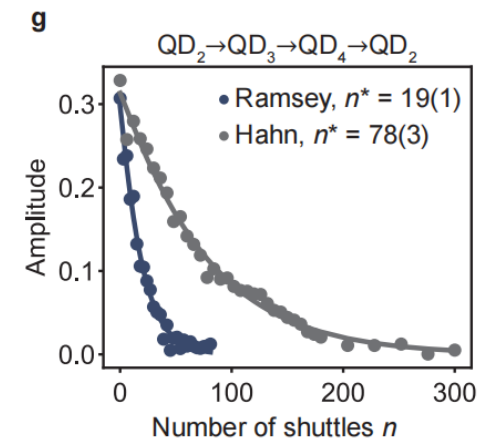
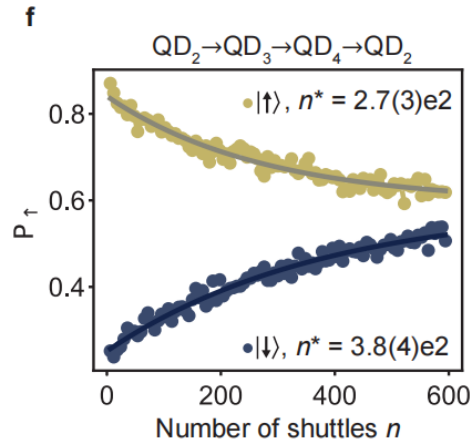
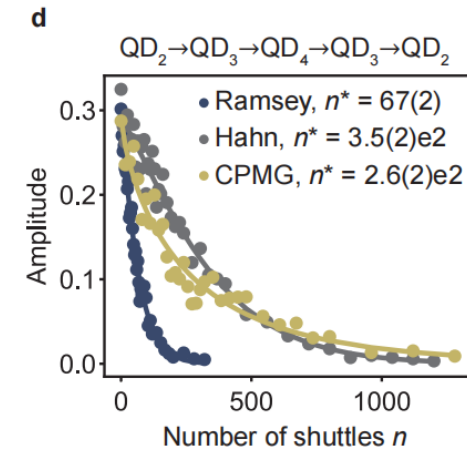
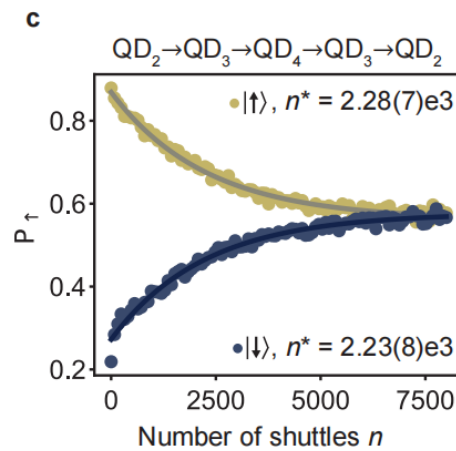
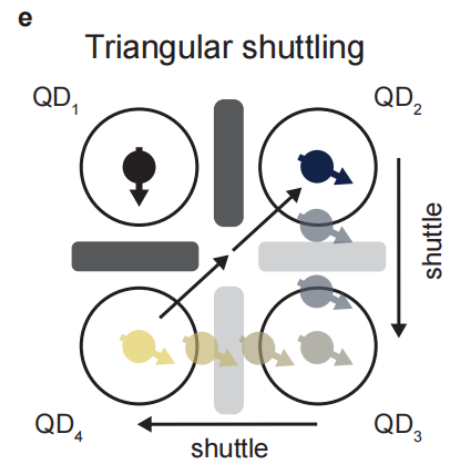
[1] Yoneda et al., Nat. Commun 12, 4114 (2021)

# Coherent Shuttling

## Free evolution experiments



QD distance = 140 nm



- Fidelity per shuttling step: 99.96% (CS) and 99.63% (TS)
- The infidelity arises from systematic error per shuttling: low coupling between QD2 and QD4,  $t_{ramp} = 36$  ns

01

Research Background

02

Electron Spin Shuttling in Si/SiGe

03

Hole Spin Shuttling in Ge/SiGe

04

Conclusions and outlooks

## Summary:

- Introduce the background of shuttling
- Characterize BB mode and CB mode shuttling in Si/SiGe
- Achieve BB mode shuttling in Ge/SiGe with strong SOI

## Outlook:

- Further research on shuttling theory
- The methods to do shuttling in NW system